Performance Analysis of the Sign Algorithm for an Adaptive IIR Notch Filter with Constrained Poles and Zeros

Naoko Tani and **Yegui Xiao**
Faculty of Human Life and Environmental Science
Hiroshima Prefectural Women's University, Hiroshima 734-8558, Japan
xiao@hirojo-u.ac.jp

Abstract *Gradient-type algorithms for adaptive IIR notch filters are very attractive in terms of both performances and computational requirements. Generally, it is quite difficult to assess their performances analytically. There have been several trials to analyze such adaptive algorithms as the sign and the plain gradient algorithms for some types of adaptive IIR notch filters, but many of them still remain unexplored. Furthermore, analysis techniques used in those trials can not be directly applied to different types of adaptive IIR notch filters.*

This paper presents a detailed performance analysis of the sign algorithm for a well-known adaptive IIR notch filter with constrained poles and zeros, which can not be done by just applying the related existing analysis techniques, and therefore has not been attempted yet. The steady-state estimation error and mean square error (MSE) of the algorithm are derived in closed forms. Stability bounds of the algorithm are also assessed. Extensive simulations are conducted to support the analytical findings.

1 Introduction

Adaptive estimation of frequency of sinusoidal signal is of essential importance in many engineering fields, such as digital communications, radar, sonar, control, biomedical engineering and so on. Adaptive IIR notch filtering for frequency estimation has attracted a lot of researchers in signal processing community, since adaptive IIR notch filters require considerably fewer filter coefficients compared with their FIR-type counterparts for the same notch bandwidth and similar performance.

There are many adaptive algorithms developed to adjust the filter coefficients of the IIR notch filters [1-6], such as the sign algorithm (SA) [2], the plain gradient algorithm (PG) [4], the normalized gradient algorithm (NG) [2], the recursive prediction error algorithm (RPE) [1], the lattice algorithm [3], the p-power algorithm [5], the memoryless nonlinear gradient algorithm [6] and so on.

Due to the IIR nature of the IIR notch filters, their performance analysis is generally much more difficult than that of their FIR counterparts, and a lot of issues therefore still remain unexplored. Nonetheless, so far, several trials have been made to analyze the performances of some of the adaptive algorithms. Petraglia et al. [7] presented some analytical results of the PG for the bilinear IIR notch filter. Although their work showed a possible way to analyze the gradient-type algorithms, the analytical results obtained from the gradient linearization is not accurate due to the bold approximations involved. Nishimura et al. [8] proposed a similar technique to analyze the performance of the SG and the PG for an IIR notch filter that is similar to the lattice notch filter in form. Their analytical results fit the simulated values reasonably well. However, it has been found that the gradient linearization techniques used by Petraglia and Nishimura can not be applied to analyze the SA and the PG for the constrained IIR notch filter [9]. The performance of the PG for the constrained IIR notch filter has been analyzed in [9], but the SA has not been considered.

This paper presents a detailed performance analysis of the SA for the constrained IIR notch filter. Difference equations governing its estimation error and MSE for the filter coefficient will be derived, assuming that, the notch filter output and the noise signal in the gradient signal, the notch filter output and the estimation error of the filter coefficient, are jointly Gaussian distributed, respectively. The steady-state bias and MSE expressions in closed form will be derived from these difference equations. Stability bounds for the step size parameter will be considered from two different standpoints. Extensive simulations will be provided to confirm the analytical results.

2 Adaptive IIR notch filter and the SA

The second-order adaptive IIR notch filter with constrained poles and zeros [1] is expressed by the following transfer function

$$H_N(z) = \frac{1 + az^{-1} + z^{-2}}{1 + \rho az^{-1} + \rho^2 z^{-2}} \tag{1}$$

where ρ is a pole contraction factor (pole radius) over $(0, 1)$ which controls the notch bandwidth of the filter. a is the filter coefficient whose true value is calculated by

$a_0 = -2\cos(\omega_0)$. ω_0 is the frequency of a noisy input sinusoidal signal

$$x(t) = A\cos(\omega_0 t + \theta) + v(t) \tag{2}$$

where $v(t)$ is an additive white Gaussian noise. θ is the phase of the signal, distributed uniformly over $[0, 2\pi)$. A is the amplitude of the sinusoid. The adaptive IIR notch filter (1) is used to estimate the frequency of the sinusoid. The SA algorithm that updates the filter coefficient is given by

$$\hat{a}(t+1) = \hat{a}(t) - \mu\ sgn(e(t))s(t) \tag{3}$$

where $sgn(\cdot)$ is a sign function. $e(t)$ is the output of the notch filter, generally referred to as error signal. μ is a step size parameter that controls the magnitude of the recursion. $\hat{a}(t)$ is the estimate of the filter coefficient a. $s(t)$, the gradient signal, is calculated by

$$s(t) = -\rho e(t-1) + x(t-1). \tag{4}$$

This SA algorithm is known to present very slow convergence but be the most cost-efficient among the many gradient-based algorithms. It may be applied to applications where slow convergence can be tolerated and implementation cost is very limited. So far, our insight into its performance is almost solely from simulation experience. It is very difficult to derive analytical expressions on the performance of this algorithm. This paper is devoted to challenging this issue.

A: Steady-state error and gradient signals

According to [9], at steady-state, the error and gradient signals may be expressed by

$$\begin{aligned} e(t) = {} & AB\delta_a(t)\cos(\omega_0 t + \theta - \phi) \\ & - \rho AB^2\delta_a^2(t)\cos(\omega_0 t + \theta - 2\phi) + v_1(t), \end{aligned} \tag{5}$$

$$\begin{aligned} s(t) = {} & A\cos(\omega_0 t + \theta - \omega_0) \\ & - \rho AB\delta_a(t)\cos(\omega_0 t + \theta - \omega_0 - \phi) \\ & + \rho^2 AB^2\delta_a^2(t)\cos(\omega_0 t + \theta - \omega_0 - 2\phi) + v_2(t) \end{aligned} \tag{6}$$

where

$$\delta_a(t) = \hat{a}(t) - a_0, \tag{7}$$

$$B = \frac{1}{(1-\rho)\sqrt{(1+\rho)^2 - 4\rho\cos^2\omega_0}}, \tag{8}$$

$$\phi = \begin{cases} \phi_0, & \omega_0 \le \dfrac{\pi}{2} \\ \pi + \phi_0, & \omega_0 > \dfrac{\pi}{2} \end{cases} \tag{9}$$

$$\phi_0 = \tan^{-1}\frac{(1+\rho)\sin\omega_0}{(1-\rho)\cos\omega_0}. \tag{10}$$

$v_1(t)$ is a zero-mean noise signal at the output of the notch filter whose variance is $\sigma_{v_1}^2$. $v_2(t)$ is also a zero-mean noise signal in the gradient signal whose variance is $\sigma_{v_2}^2$. The correlation between these two noise signals is indicated by $R_{1,2}$. See [9] for their calculations.

3 Performance analysis

In this section, first, two difference equations for the estimation bias and MSE of the filter coefficient will be established. Then, the steady-state estimation error and MSE will be derived. Finally, stability bounds will also be considered from two points of view.

A: Estimation bias

Using (5-7) in (3), the difference equation for convergence in the mean for the estimation error $\delta_a(t)$ can be expressed as

$$\begin{aligned} & E[\delta_a(t+1)] \\ & = E[\delta_a(t)] - \mu A\cos(\omega_0 t + \theta - \omega_0)\underbrace{E[sgn(e(t))]}_{=I_1(t)} \\ & \quad + \mu\rho AB\cos(\omega_0 t + \theta - \omega_0 - \phi)\underbrace{E[sgn(e(t))\ \delta_a(t)]}_{=I_2(t)} \\ & \quad - \mu\rho^2 AB^2\cos(\omega_0 t + \theta - \omega_0 - 2\phi)\underbrace{E[sgn(e(t))\ \delta_a^2(t)]}_{=I_3(t)} \\ & \quad - \mu\underbrace{E[sgn(e(t))\ v_2(t)]}_{=I_4(t)}. \end{aligned} \tag{11}$$

To calculate $I_1(t)$, $I_2(t)$, $I_3(t)$, and $I_4(t)$, we need to have further information on the probability distribution of $e(t)$, probabilistic relations between $e(t)$ and $\delta_a(t)$, and between $e(t)$ and $v_2(t)$. When $v(t)$ is Gaussian distributed, we have found that $e(t)$ follows the Gaussian distribution, and $e(t)$ and $\delta_a(t)$, $e(t)$ and $v_2(t)$, are jointly Gaussian distributed, respectively. Mathematical details are omitted due to space limitation. Following these findings, we have, after very complicated and technical calculations,

$$I_1(t) = 2sgn\left(\frac{\mu_e}{\sigma_e}\right) erf\left(\left|\frac{\mu_e}{\sigma_e}\right|\right), \tag{12}$$

$$\begin{aligned} I_2(t) = {} & 2E[\delta_a(t)]sgn\left(\frac{\mu_e}{\sigma_e}\right) erf\left(\left|\frac{\mu_e}{\sigma_e}\right|\right) \\ & + \sqrt{\frac{2}{\pi}}\frac{Q_{e\delta_a}}{\sigma_e}\exp\left\{-\frac{1}{2}\left(\frac{\mu_e}{\sigma_e}\right)^2\right\}, \end{aligned} \tag{13}$$

$$\begin{aligned} I_3(t) = {} & 2\frac{|[Q]|}{Q_e}sgn\left(\frac{\mu_e}{\sigma_e}\right) erf\left(\left|\frac{\mu_e}{\sigma_e}\right|\right) \\ & + 2E^2[\delta_a(t)]sgn\left(\frac{\mu_e}{\sigma_e}\right) erf\left(\left|\frac{\mu_e}{\sigma_e}\right|\right) \\ & + 2E[\delta_a(t)]\frac{Q_{e\delta_a}}{\sigma_e}\sqrt{\frac{2}{\pi}}\exp\left\{-\frac{1}{2}\left(\frac{\mu_e}{\sigma_e}\right)^2\right\} \\ & - \frac{Q_{e\delta_a}^2}{\sigma_e^3}\sqrt{\frac{2}{\pi}}\,\mu_e\exp\left\{-\frac{1}{2}\left(\frac{\mu_e}{\sigma_e}\right)^2\right\} \\ & + \frac{Q_{e\delta_a}^2}{Q_e}\,2sgn\left(\frac{\mu_e}{\sigma_e}\right) erf\left(\left|\frac{\mu_e}{\sigma_e}\right|\right), \end{aligned} \tag{14}$$

$$I_4(t) = \frac{R_{1,2}}{\sigma_e}\sqrt{\frac{2}{\pi}}\exp\left\{-\frac{1}{2}\left(\frac{\mu_e}{\sigma_e}\right)^2\right\}. \tag{15}$$

In the derivations of (12)—(15), it is also assumed that $\delta_a(t)$ and $v_1(t)$, $\delta_a(t)$ and $v_2(t)$ are uncorrelated to each

other, respectively. Furthermore, terms of $\delta_a(t)$ with orders equal to or higher than 3 are ignored for analytical simplicity. Explanations to several variables such as $erf(\cdot)$, $Q_{e\delta_a}$, etc. in (12)—(15) are omitted to save space. Substituting (12)—(15) back to (11) and ignoring many insignificant terms, one ultimately has

$$E[\delta_a(t+1)] = (1-\mu\psi_{11})\,E[\delta_a(t)] + \mu\psi_{12}E[\delta_a^2(t)] + \mu\eta_1 \tag{16}$$

where

$$\psi_{11} = \frac{A^2B}{\sqrt{2\pi}\sigma_{v_1}}\cos(\omega_0-\phi), \tag{17}$$

$$\psi_{12} = \frac{\rho A^2B^2}{\sqrt{2\pi}\sigma_{v_1}}\{\cos(\omega_0-2\phi)+\cos\omega_0\}, \tag{18}$$

$$\eta_1 = -\sqrt{\frac{2}{\pi}}\frac{R_{1,2}}{\sigma_{v_1}}\,. \tag{19}$$

B: Estimation MSE

From (3) and (7), we have

$$E[\delta_a^2(t+1)] = E[\delta_a^2(t)] - 2\mu\underbrace{E[\delta_a(t)sgn(e(t))s(t)]}_{=M_1(t)} + \mu^2\underbrace{E[s^2(t)]}_{=M_2(t)}\,. \tag{20}$$

After very complicated calculations, $M_1(t)$ and $M_2(t)$ can be worked out under the assumptions used in the derivations of (12)—(15), as follows

$$\begin{aligned} M_1(t) = A\Bigg[& 2E[\delta_a(t)]sgn\left(\frac{\mu_e}{\sigma_e}\right)erf\left(\left|\frac{\mu_e}{\sigma_e}\right|\right) \\ & +\sqrt{\frac{2}{\pi}}\frac{Q_{e\delta_a}}{\sigma_e}\exp\left\{-\frac{1}{2}\left(\frac{\mu_e}{\sigma_e}\right)^2\right\}\Bigg] \\ & \times\cos(\omega_0t+\theta-\omega_0) \\ & -\rho AB\Bigg[2\frac{|[Q]|}{Q_e}sgn\left(\frac{\mu_e}{\sigma_e}\right)erf\left(\left|\frac{\mu_e}{\sigma_e}\right|\right) \\ & +2E^2[\delta_a(t)]sgn\left(\frac{\mu_e}{\sigma_e}\right)erf\left(\left|\frac{\mu_e}{\sigma_e}\right|\right) \\ & +2E[\delta_a(t)]\frac{Q_{e\delta_a}}{\sigma_e}\sqrt{\frac{2}{\pi}}\exp\left\{-\frac{1}{2}\left(\frac{\mu_e}{\sigma_e}\right)^2\right\} \\ & -\frac{Q_{e\delta_a}^2}{\sigma_e^3}\sqrt{\frac{2}{\pi}}\mu_e\exp\left\{-\frac{1}{2}\left(\frac{\mu_e}{\sigma_e}\right)^2\right\} \\ & +\frac{Q_{e\delta_a}^2}{Q_e}2sgn\left(\frac{\mu_e}{\sigma_e}\right)erf\left(\left|\frac{\mu_e}{\sigma_e}\right|\right)\Bigg] \\ & \times\cos(\omega_0t+\theta-\omega_0-\phi) \\ & +E[\delta_a(t)]\,\frac{R_{1,2}}{\sigma_e}\sqrt{\frac{2}{\pi}}\exp\left\{-\frac{1}{2}\left(\frac{\mu_e}{\sigma_e}\right)^2\right\}, \end{aligned} \tag{21}$$

$$\begin{aligned} M_2(t) = {} & A^2\cos^2(\omega_0t+\theta-\omega_0) \\ & +\rho^2A^2B^2E[\delta_a^2(t)]\cos^2(\omega_0t+\theta-\omega_0-\phi) \\ & +\sigma_{v_2}^2 \\ & -2\rho A^2BE[\delta_a(t)]\cos(\omega_0t+\theta-\omega_0) \\ & \times\cos(\omega_0t+\theta-\omega_0-\phi) \\ & +2\rho^2A^2B^2E[\delta_a^2(t)]\cos(\omega_0t+\theta-\omega_0) \\ & \times\cos(\omega_0t+\theta-\omega_0-2\phi)\,. \end{aligned} \tag{22}$$

Putting (21) and (22) back into (20) and removing the insignificant terms, we get the difference equation for the convergence in the mean square, as follows

$$E[\delta_a^2(t+1)] = -\mu\psi_{21}E[\delta_a(t)] + (1-\mu\psi_{22})E[\delta_a^2(t)] + \mu^2\eta_2 \tag{23}$$

where

$$\psi_{21} = \sqrt{\frac{2}{\pi}}\frac{2R_{1,2}}{\sigma_{v_1}}, \tag{24}$$

$$\psi_{22} = \sqrt{\frac{2}{\pi}}\frac{A^2B}{\sigma_{v_1}}\cos(\omega_0-\phi), \tag{25}$$

$$\eta_2 = \frac{1}{2}A^2+\sigma_{v_2}^2\,. \tag{26}$$

C: Steady-state estimation bias and MSE

Next, we consider the steady-state estimation bias and MSE, utilizing the difference equations for the convergences in the mean and mean square that we have established above. At steady-state, using $E[\delta_a(t+1)]|_{t\to\infty} = E[\delta_a(t)]|_{t\to\infty} = E[\delta_a(\infty)]$ and $E[\delta_a^2(t+1)]|_{t\to\infty} = E[\delta_a^2(t)]|_{t\to\infty} = E[\delta_a^2(\infty)]$ in (16) and (23), and solving the resultant equations as simultaneous equations, we reach

$$E[\delta_a(\infty)] = \frac{\mu\eta_2\psi_{12}+\eta_1\psi_{22}}{\psi_{11}\psi_{22}+\psi_{12}\psi_{21}}\,, \tag{27}$$

$$E[\delta_a^2(\infty)] = \frac{\mu\eta_2\psi_{11}-\eta_1\psi_{21}}{\psi_{11}\psi_{22}+\psi_{12}\psi_{21}}\,. \tag{28}$$

These are the closed form expressions for the steady-state estimation error (bias) and MSE.

D: Stability bounds

Here, we move to the next step to derive stability bounds for the step size parameter, now that we have established the difference equations for the convergences in the mean and in the mean square.

(a) Stability bound A

Putting (16) and (23) together, a simultaneous difference equation set can be produced. Allowing the eigenvalue to be $\lambda=-1$ results in a second-order equation about the step size parameter μ, and its solutions are

$$\mu_{1,2} = \frac{(\psi_{11}+\psi_{22}) \pm \sqrt{(\psi_{11}-\psi_{22})^2-4\psi_{12}\psi_{21}}}{\psi_{11}\psi_{22}+\psi_{12}\psi_{21}}\,. \tag{29}$$

A meaningful stability bound can be easily derived from the above equation.

(b) Stability bound B

If we ignore the influence of the estimation bias in (23), then $|1-\mu\psi_{22}|<1$ must be satisfied to ensure the convergence of the algorithm in the mean square sense. This readily leads to the following stability bound

$$0<\mu<\frac{2}{\psi_{22}}\ . \tag{30}$$

On the other hand, if we ignore the influence of the MSE in (16), then $|1-\mu\psi_{11}|<1$ must be satisfied to ensure the convergence of the algorithm in the mean sense. This gives another stability bound

$$0<\mu<\frac{2}{\psi_{11}}\ . \tag{31}$$

Therefore one more stability bound may be obtained by selecting the smaller one from (30) and (31).

D Simulation results

Here, we show some typical simulation results. Fig.1 shows comparisons between the theory and simulation for the estimation bias and MSE versus the pole radius ρ. It can be noticed that the analytical estimation bias expression presents excellent fit to the simulated values over the entire range of ρ. It is also clear that the analytical estimation MSE also fits the simulation very well on the whole.

Fig.2 presents comparisons between the two theoretical stability bounds obtained from (29)—(30) with their simulated values. Although there are some differences between them, the two theoretical stability bounds provide good estimates on the whole for the simulated stability bound of the algorithm when the additive noise is not large.

4 Conclusions

In this paper, closed form expressions for the steady-state estimation bias, the MSE and the stability bounds have been derived for the SA updating the second-order IIR notch filter with constrained poles and zeros. Simulation results have been shown to indicate the effectiveness of the analytical expressions. Tracking analysis of the SA is an open topic for further explorations.

References

[1] A. Nehorai, *"A minimal parameter adaptive notch filter with constrained poles and zeros,"* IEEE Trans. Acoust., Speech, Signal Processing, vol.ASSP-33, No.4, pp.983-996(1985).

[2] K. Martin and M. T. Sun, *"Adaptive filters suitable for real-time spectral analysis,"* IEEE Trans. Circuits, Syst., vol.CAS-33, No.2, pp.218-229(1986).

[3] N. I. Cho and S. U. Lee, *"On the adaptive lattice notch filter for the detection of sinusoids,"* IEEE Trans. Circuits, Syst., vol.40, No.7, pp.405-416(1993).

[4] J. F. Chicharo and T. S. Ng, *"Gradient-based adaptive IIR notch filtering for frequency estimation,"* IEEE Trans. Acoust., Speech, Signal Processing, vol.ASSP-38, No.5, pp.769-777(1990).

[5] S.-C. Pei, and C.-C. Tseng, *"Adaptive IIR notch filter based on least mean p-power error criterion,"* IEEE Trans. on Circuits, Syst., vol.40, No.8, pp.525-529(1993).

[6] Y. Xiao, Y. Kobayashi, and Y. Tadokoro, *"A new memoryless nonlinear gradient algorithm for a second-order adaptive IIR notch filter and its performance analysis,"* IEEE Trans. on Circuits, Syst., vol.45, No.4, pp.462-472(1998).

[7] Mariane R. Petraglia, John J. Shynk, and Sanjit K. Mitra *"Stability bounds and steady-state coefficient variance for a second-order adaptive IIR notch filter,"* IEEE Trans. Signal Processing., vol.42, No.7, pp.1841-1845(1994).

[8] S. Nishimura, J. K. Kim, and K. Hirano, *"Mean-squared error analysis of an adaptive notch filter,"* in Proc. IEEE Int. Symp. Circuits, Syst. (Portland, OR), pp.732-735(1989).

[9] Y. Xiao, Y. Takeshita, and K. Shida, *"Performance analysis of a gradient-based second-order adaptive IIR notch filter with constrained poles and zeros,"* Proceedings of ITC-CSCC'99, Vol.1, pp.541-544(1999); also submitted to IEEE Trans. on Circuits, Syst.(1999).

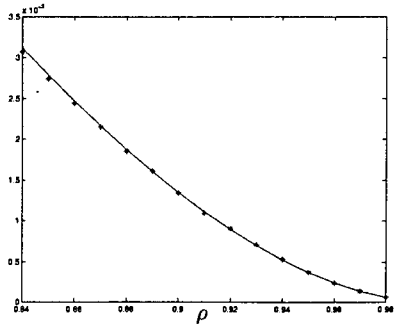

(a) Estimation bias

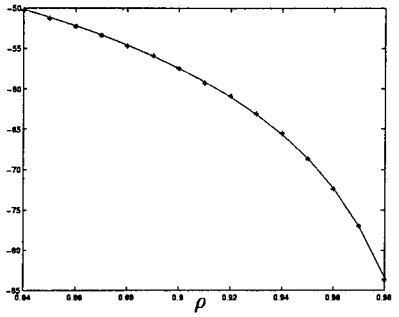

(b) Estimation MSE

Fig.1 Comparisons between theory and simulations versus ρ ; theory: solid line, simulation: star, ($\mu = 1.0\times10^{-7}$, $\omega_0 = 0.2\pi$, $SNR = 10[dB]$, $A=\sqrt{2}$, $\theta=\frac{\pi}{6}$, 100 *runs*) .

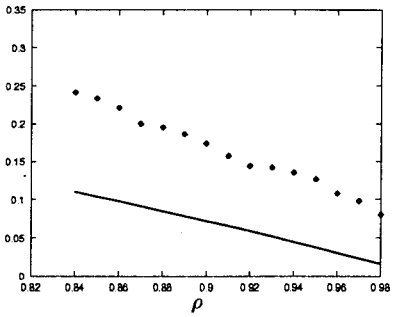

Stability bound

Fig.2 Comparisons between theory and simulations versus ρ for the stability bounds; theory: solid line, simulation: diamond, ($\omega_0 = 0.2\pi$, $SNR = 10[dB]$, $A=\sqrt{2}$, $\theta=\frac{\pi}{6}$, 100 *runs*) .